Type I IFN suppresses Cxcr2 driven neutrophil recruitment into the sensory ganglia during viral infection

Angus T. Stock,[1,2] Jeffrey M. Smith,[1] and Francis R. Carbone[1]

[1]Department of Microbiology and Immunology, Peter Doherty Institute for Infection and Immunity, the University of Melbourne, Parkville, Victoria 3010, Australia
[2]The Walter and Eliza Hall Institute of Medical Research, Melbourne, Parkville, Victoria 3052, Australia

Infection induces the expression of inflammatory chemokines that recruit immune cells to the site of inflammation. Whereas tissues such as the intestine and skin express unique chemokines during homeostasis, whether different tissues express distinct chemokine profiles during inflammation remains unclear. With this in mind, we performed a comprehensive screen of the chemokines expressed by two tissues (skin and sensory ganglia) infected with a common viral pathogen (herpes simplex virus type 1). After infection, the skin and ganglia showed marked differences in their expression of the family of Cxcr2 chemokine ligands. Specifically, Cxcl1/2/3, which in turn controlled neutrophil recruitment, was up-regulated in the skin but absent from the ganglia. Within the ganglia, Cxcl2 expression and subsequent neutrophil recruitment was inhibited by type I interferon (IFN). Using a combination of bone marrow chimeras and intracellular chemokine staining, we show that type I IFN acted by directly suppressing Cxcl2 expression by monocytes, abrogating their ability to recruit neutrophils to the ganglia. Overall, our findings describe a novel role for IFN in the direct, and selective, inhibition of Cxcr2 chemokine ligands, which results in the inhibition of neutrophil recruitment to neuronal tissue.

CORRESPONDENCE
Angus T. Stock:
stock.a@wehi.edu.au
OR
Francis R. Carbone:
fcarbone@unimelb.edu.au

Abbreviations used: DRG, dorsal root ganglia; HSV-1, HSV type 1; p.i., postinfection.

How immune cells move from circulation into tissue is now well defined. This is a sequential process where lectins or integrins facilitate the initial rolling of cells on the endothelial wall. In this state, cells are exposed to locally produced chemokines that trigger integrin activation and cell polarization, thus enabling integrin-mediated firm arrest and extravasation into the tissue (Butcher and Picker, 1996).

Despite serving a common function (i.e., cell migration), the chemokine family is incredibly diverse. There are almost 50 human chemokines (~38 murine) that collectively serve as ligands for 18 functional G protein–coupled receptors (Zlotnik and Yoshie, 2012). The chemokine family is divided by structure and kinetics of expression, being split into four groups (CC, CXC, CX3C, and XC) based upon the arrangement of N-terminal cysteines, and further divided between homeostatic (expressed during homeostasis), inflammatory (expressed during inflammation), and dual chemokines (expressed in steady state and inflammation; Zlotnik and Yoshie, 2012). In regard to receptors, diversity in chemokine receptor expression is observed between and within immune cell subsets. For instance, neutrophils (Cxcr1/2) and monocytes (Ccr2) use distinct chemokine receptors to facilitate migration (Shuster et al., 1995; Serbina et al., 2008), whereas the $CD4^+$ T cell subsets T_h1 (Cxcr3 and Ccr5), T_h2 (Ccr4 and Ccr8), T_h17 (Ccr6), and T_fh (Cxcr5) cells are all associated with unique chemokine receptor usage, and thus respond to different ligands (Sallusto and Lanzavecchia, 2009).

An intriguing feature of the chemokine family is that certain members exhibit tissue-specific expression patterns. Notably, Ccl19 and Ccl21 (ligands for Ccr7) are expressed mainly within the lymphoid compartment (Cyster, 2005), Ccl25 (ligand for Ccr9) is expressed by the thymus and small intestine (Svensson et al., 2002), and Ccl27 (ligand for Ccr10) is expressed in skin (Reiss et al., 2001). It is generally agreed that tissue-specific chemokines enable targeted migration patterns.

The Rockefeller University Press $30.00
J. Exp. Med. 2014 Vol. 211 No. 5 751–759
www.jem.org/cgi/doi/10.1084/jem.20132183

The Journal of Experimental Medicine

However, although this concept is well accepted, it is important to note that these putative tissue-specific ligands are homeostatic chemokines. As such, whether different tissues continue to express unique chemokine profiles during periods of inflammation remains to be seen. Given that pathogens commonly infect multiple organs during their lifecycle, whether differing tissues express a conserved or distinct chemokine profile during infection is an important question. Furthermore, considering that some inflammatory chemokines selectively recruit specific immune cell subsets, differential chemokine expression may enable tissues to tailor immune cell recruitment to complement the requirements of particular organs. Here, we have examined this issue in the context of HSV type I (HSV-1). This pathogen typically causes an orofacial infection in humans, replicating in the skin epithelia and innervating trigeminal ganglia, and therefore provides an ideal model to examine whether two tissues (skin and ganglia) express similar or distinct chemokine profiles during infection with a common pathogen.

RESULTS AND DISCUSSION

The skin, but not sensory ganglia, expresses Cxcr2 chemokine ligands and activates neutrophil recruitment after HSV-1 infection

Here, we used a mouse model of epicutaneous flank HSV-1 infection. Upon infection, virus travels to the innervating dorsal root ganglia (DRG), infecting neurons within the ganglia, and then returns to infect distal regions of skin (secondary site) throughout the dermatome within 2–3 d of inoculation (van Lint et al., 2004). Using a comprehensive real-time PCR array, we measured chemokine expression in the secondary site skin (hereafter referred to as skin) and DRG at day 5 postinfection (p.i.), when viral loads are at their peak in both tissues (van Lint et al., 2004). As seen in Fig. 1, although several inflammatory chemokines (Ccl2/5/7 and Cxcl9/10) increased in both skin and DRG after infection, there was a marked differential expression of the family of Cxcr2 chemokine ligands Cxcl1/2/3 between the two sites. Most notably, Cxcl2 mRNA expression increased dramatically (~1000 fold) in the skin after HSV-1 infection, but was largely absent from the DRG (Fig. 1 a). Consistent with mRNA expression, although Ccl2 protein levels increased in both skin and DRG after infection, Cxcl2 protein was abundant in the skin beyond day 4, but undetectable in the DRG at all time points tested (Fig. 1 b).

Cxcl2 belongs to a family of chemokines that serve as ligands for Cxcr2 (Addison et al., 2000), a chemokine receptor highly expressed by neutrophils (Shuster et al., 1995). In line with Cxcl1/2/3 expression controlling neutrophil recruitment, large numbers of $CD11b^+Ly6G^+$ neutrophils migrated into infected skin, peaking at day 6 p.i., but were largely absent from DRG at all time-points tested (Fig. 1 c). In contrast, $CD11b^+Ly6C^+$ monocytes migrated to both skin and ganglia after infection, in line with the common expression of the Ccr2 ligands Ccl2 and Ccl7 (Fig. 1 a). $Ly6G^+$ neutrophils were concentrated at the base of the infected epidermis in the skin (Fig. 1 d), but were again not detected within the infected DRG by microscopy, despite the appearance of $Ly6C^+$ monocytes at this site.

To test if Cxcr2 chemokines were driving skin neutrophil recruitment, we transferred donor BM in combination with a Cxcr2 blocking antibody into infected mice, and tracked the migration of donor BM monocytes and neutrophils into the skin (anti–Gr-1 antibody was injected just before sacrifice to discriminate between circulating [in vivo–labeled] and tissue-resident [nonlabeled] cells; Ng et al., 2011). As seen in Fig. 1 e, although donor neutrophil frequency in the spleen was comparable between groups, the migration of donor neutrophils, but not monocytes, into the skin was greatly impaired by Cxcr2 blocking. Intriguingly, myeloid cells were the dominant producers of Cxcl2 in the skin, as both $Ly6G^+$ neutrophils and $Ly6C^+$ monocytes stained strongly for intracellular Cxcl2 (Fig. 1 f). Furthermore, Cxcl2 mRNA was abundant in neutrophils, and to a lesser extent monocyte/macrophages sorted from HSV-1–infected skin (Fig. 1 g), but was absent from lymphoid and parenchymal cells. Collectively, these findings show that (a) Cxcr2 ligands, expressed by neutrophils and monocytes, drive neutrophil recruitment to the skin after HSV-1 infection, and (b) Cxcl1/2/3 is not expressed within the DRG, preventing neutrophil recruitment to this site. To our knowledge, this is the first description of differential expression of inflammatory chemokines in distinct tissues involved in the same infection, and argues that skin and ganglia differentially regulate Cxcr2 chemokine ligands to promote or inhibit neutrophil recruitment, respectively.

Type I IFN signaling through the hematopoietic cells suppresses neutrophil recruitment into ganglia after HSV infection

We were surprised that, in the face of viral infection, the ganglia could simultaneously recruit monocytes and exclude neutrophils. Given the report that neutrophil infiltration correlates the infection virulence (Brandes et al., 2013), we wondered whether neutrophils would infiltrate the ganglia when infected with a more virulent and/or poorly controlled infection. To test this, we measured DRG neutrophil infiltration after infection with a highly virulent HSV strain (SC16), or when mice were deficient in components of the immune system. Surprisingly, we observed minimal neutrophil infiltrate in the ganglia of B6 mice infected with SC16 HSV, or to the DRG of RAG-$\gamma C^{-/-}$, $CCR2^{-/-}$, $MyD88^{-/-}$, or $TLR3^{-/-}$ mice infected with HSV-KOS (Fig. 2 a). All combinations of virus and/or knockout lead to exaggerated, and in most cases, lethal infection (Ashkar and Rosenthal, 2003). Thus, even in the face of neurovirulent infections, neutrophils are restricted from migrating to the sensory ganglia.

In contrast, type I IFN receptor–deficient mice ($Ifn\alpha R^{-/-}$) had massive DRG neutrophil infiltration after wild-type HSV-1 infection, as did infected B6 mice treated with an anti-IFNαR blocking antibody. $IFN\gamma^{-/-}$ mice also had moderately increased neutrophilia, suggesting a common IFN-mediated phenomenon (Fig. 2 a). Although $Ifn\alpha R^{-/-}$ mice are known to poorly control wild-type HSV-1 (Halford et al., 1997), defective control itself was insufficient to prompt neutrophil recruitment in other knockout strains. Furthermore, monocyte recruitment

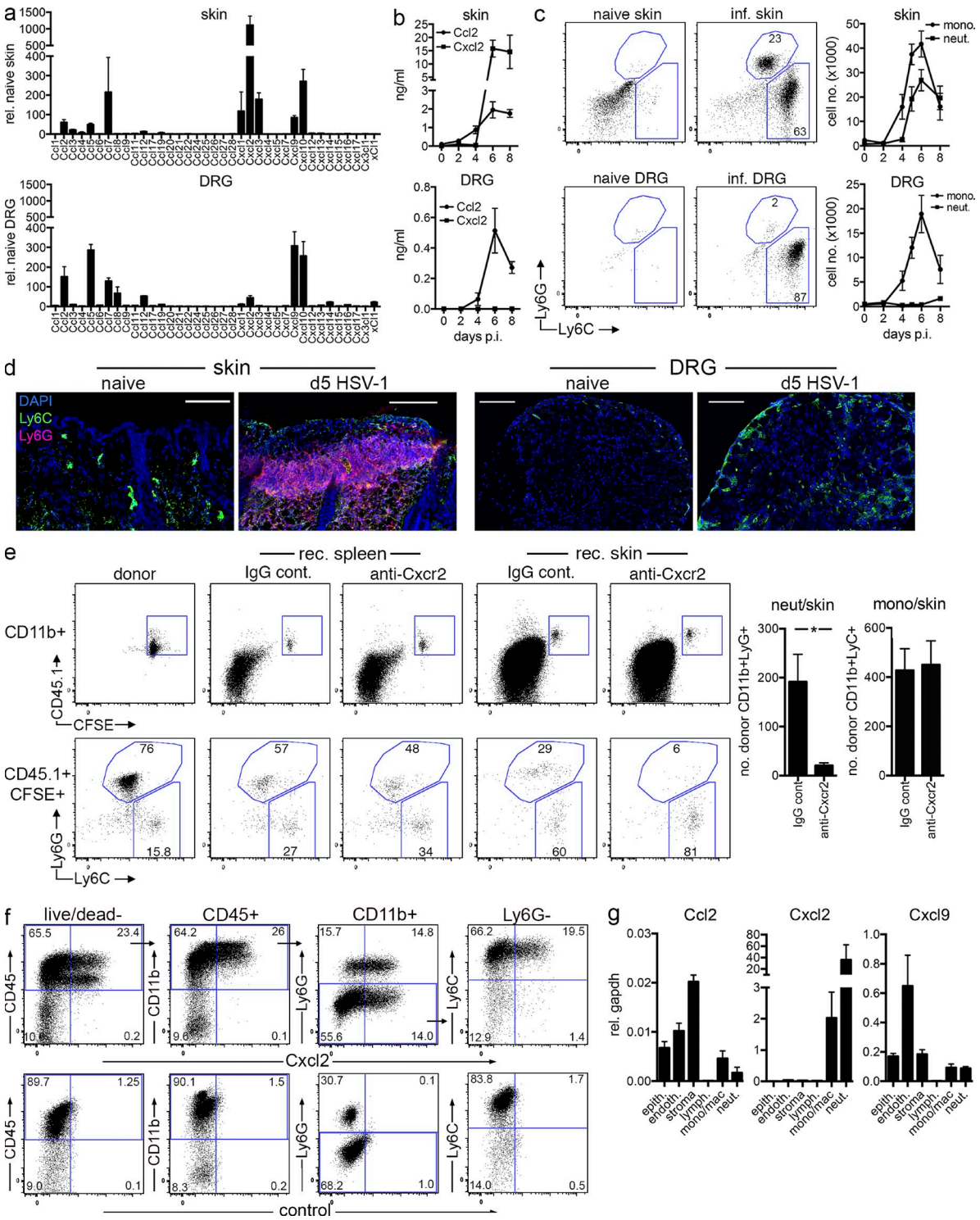

Figure 1. Differential Cxcl1/2/3 expression and neutrophil recruitment by the skin and ganglia after HSV-1 infection. (a) B6 mice were infected with HSV-1 and, 5 d later, chemokine expression was measured in the skin and DRG by qPCR (values are relative to naive tissue). (b and c) After infection, tissues were harvested and (b) Cxcl2 and Ccl2 measured by ELISA or (c) the number of neutrophils ($CD11b^+/Ly6G^+$) and monocytes ($CD11b^+/Ly6C^+$) determined by FACs. Plots (gated on $CD11b^+PI^-$) are of naive or day 5 infected mice. (d) Skin and DRG sections stained for Ly6C (green), Ly6G (magenta), and DAPI. Bars, 100 µm. (e) $CD45.1^+CFSE^+$ BM cells were transferred with anti-Cxcr2 or IgG antibody into day 5–6–infected B6 mice. After 2 h, mice received anti–Gr-1 PE to label circulating granulocytes and were sacrificed 10 min later. The number of tissue-resident ($Gr\text{-}1^-$) donor ($CFSE^+/CD45.1^+$) neutrophils ($CD11b^+/Ly6G^+$) and monocytes ($CD11b^+/Ly6C^+$) in the skin, or $GR\text{-}1^{+/-}$ donor cells in the spleen was determined by FACs. (f and g) Skin from day 6 HSV-1–infected B6 mice was (f) stained ex vivo for intracellular Cxcl2 (or isotype control) or (g) sorted into cell subsets for qPCR analysis. Data in a–g are mean (±SEM) of 6–33 mice per group, acquired from at least two independent experiments. *, $P < 0.05$ (unpaired Student's *t* test).

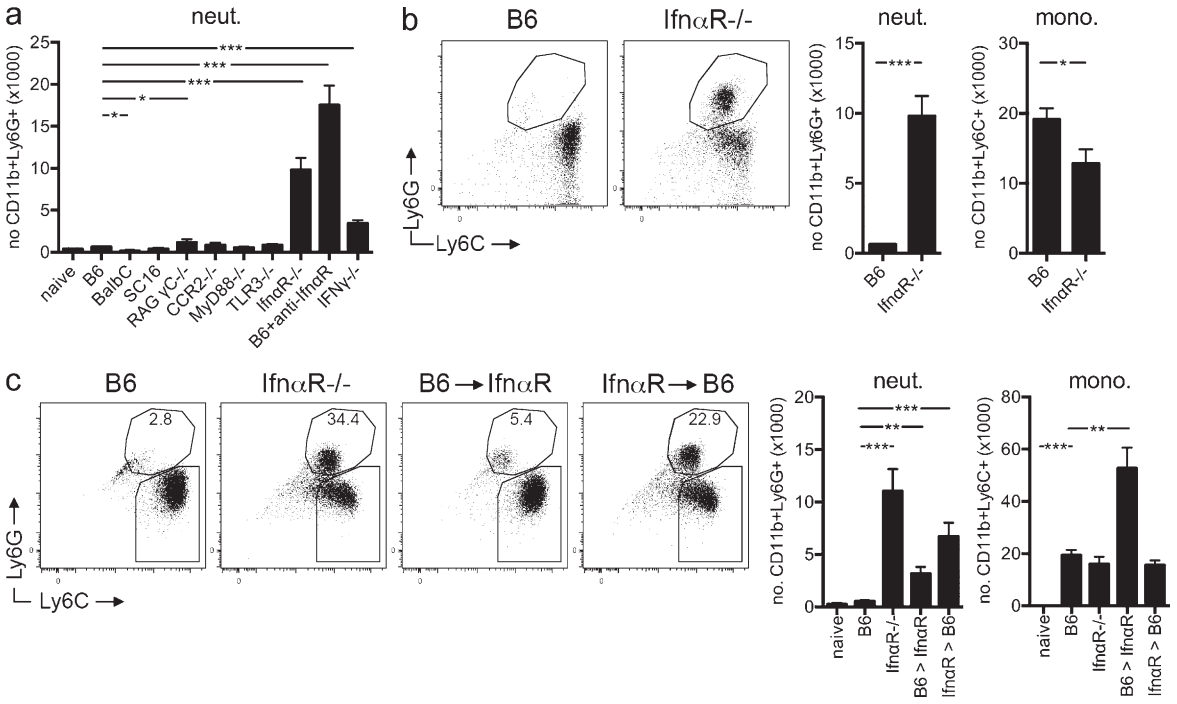

Figure 2. Type I IFN signaling through hematopoietic cells suppresses neutrophil recruitment to the ganglia. (a) Mice were infected with HSV-1 and at day 5–6 p.i., the number of neutrophils infiltrating the DRG was determined by FACs (SC16 represents B6 mice infected with the SC16 HSV, and B6+α-IfnαR, KOS-infected B6 mice treated with anti-IfnaR ab). (b and c) B6, IfnαR$^{-/-}$, or BM chimeras were infected with HSV-1 and at day 5 p.i. The DRG was analyzed by FACs. Plots are gated on CD11b^{+}PI^{-} events and data in a–c are mean (±SEM) of 6–61 mice per group, pooled from at least 2 independent experiments. *, P < 0.05; **, P < 0.001; ***, P < 0.0001 (unpaired Student's *t* Test).

into the DRG of IfnαR$^{-/-}$ mice was largely equivalent to wild-type mice (Fig. 2 b), arguing against a global increase in leukocyte recruitment. Thus, IFN signaling appeared to selectively inhibit neutrophil recruitment in the ganglia.

We subsequently examined whether type I IFN signaled through the hematopoietic or parenchymal compartment to restrict neutrophil migration. To this end, we infected B6.Ly5.1 → IfnαR$^{-/-}$ and IfnαR$^{-/-}$ → B6.Ly5.1 BM chimeras with HSV-1 and measured neutrophil and monocyte migration into the DRG. As seen in Fig. 2c, although B6.Ly5.1 → IfnαR$^{-/-}$ chimeras showed an increase in neutrophil infiltration, IfnαR$^{-/-}$ → B6.Ly5.1 chimeras entirely recapitulated the IfnαR$^{-/-}$ phenotype, with robust neutrophil recruitment into the DRG and no impact upon monocyte levels. These results indicate that type I signaling on radiosensitive hematopoietic cells suppresses the recruitment of neutrophils to the ganglia during infection.

Type I IFN signaling blocks Cxcr2-driven neutrophil recruitment to the ganglia by inhibiting the production of Cxcl2 by monocytes

DRG recruitment of neutrophils in the absence of type I IFN signaling was associated with the increased expression of the Cxcr2 chemokine ligands. HSV-infected IfnαR$^{-/-}$ mice had highly elevated levels of Cxcl1/2/3 compared with B6 counterparts, while maintaining normal expression of Ccl2/7 within the DRG (Fig. 3 a). To confirm that Cxcl1/2/3 expression was driving neutrophil recruitment in IfnαR$^{-/-}$ mice, we examined whether Cxcr2 blocking impaired neutrophil entry to the DRG. To this end, we transferred donor BM in combination with a Cxcr2 blocking antibody into HSV-1–infected IfnαR$^{-/-}$ mice, and measured donor monocyte/neutrophil migration into the DRG. As seen in Fig. 3 b, the migration of donor neutrophils, but not monocytes, was significantly impaired by Cxcr2 blocking. Thus, neutrophil migration into IfnαR$^{-/-}$ DRG is Cxcr2 dependent, and most likely in response to Cxcl1/2/3 expression.

To identify the source of Cxcr2 chemokine ligands, we isolated DRG from infected mice and stained directly ex vivo for intracellular Cxcl2. Although the B6 DRG was devoid of Cxcl2^{+} cells, a large fraction of CD45^{+}CD11b^{+} leukocytes isolated from the IfnαR$^{-/-}$ DRG were producing Cxcl2 (Fig. 3 c). Additional profiling showed that the highest producers of Cxcl2 within the IfnαR$^{-/-}$ ganglia were CD45^{+}CD11b^{+}Ly6G^{-} Ly6C^{+}-infiltrating monocytes. Furthermore, monocytes sorted from the DRG of infected IfnαR$^{-/-}$ mice had elevated Cxcl2 mRNA compared with their B6 counterparts (Fig. 3 e). Of note, splenic monocytes did not stain for Cxcl2, and had little Cxcl2 mRNA, indicating that monocytes up-regulate Cxcl2 only after DRG entry (Fig. 3, d and e). Collectively, these results indicate that type I IFN signaling blocks Cxcl2 expression by monocytes within the ganglia, thereby disabling neutrophil recruitment.

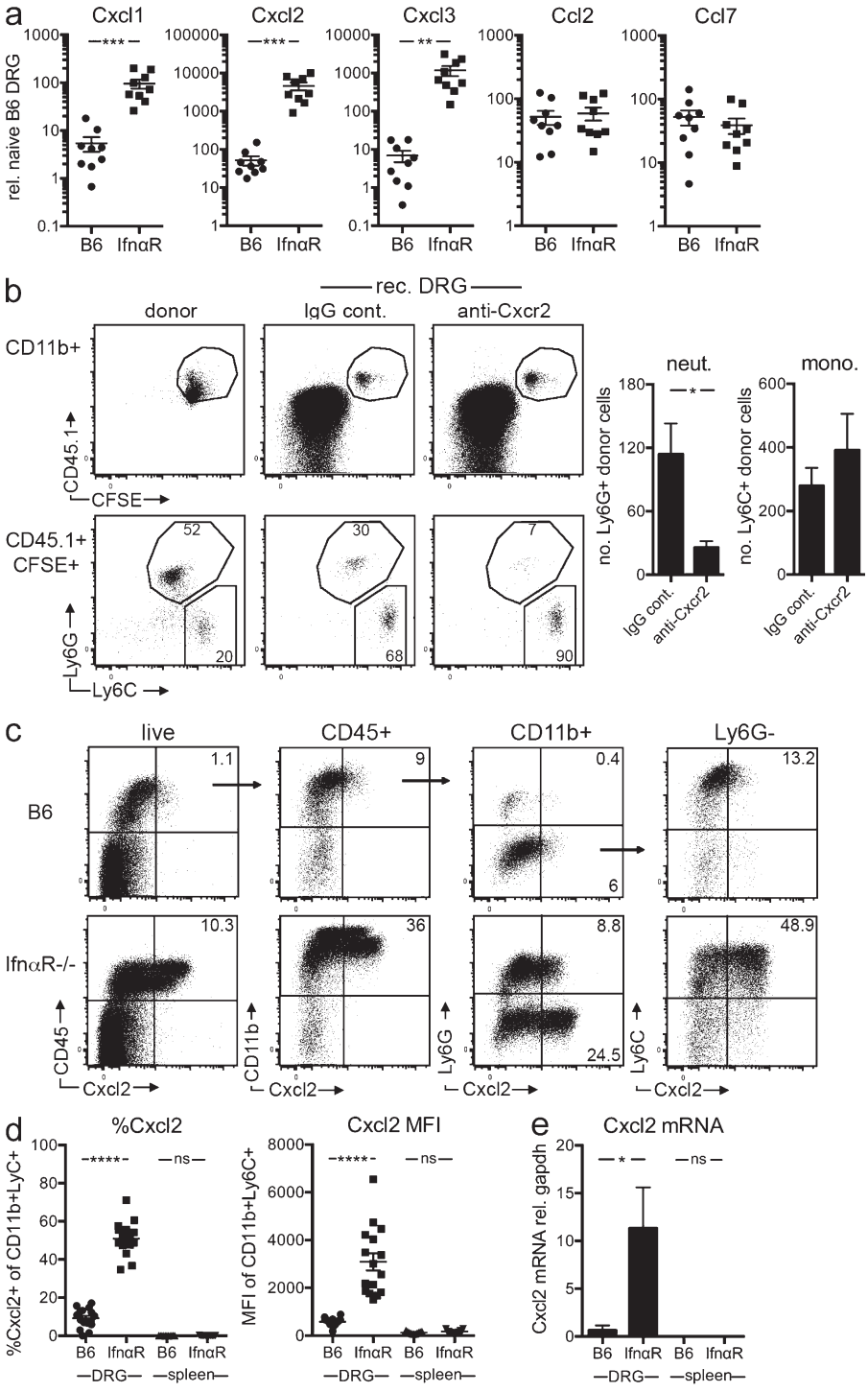

Figure 3. Cxcr2-dependent neutrophil recruitment to the ganglia is driven by Cxcl2-producing monocytes. (a) B6 or IfnαR$^{-/-}$ mice were infected with HSV-1 and at day 5 p.i., the DRG isolated for chemokine analysis by qPCR. Dots are individual mice pooled from three experiments. (b) CFSE^{+} CD45.1^{+} BM was transferred into infected IfnαR$^{-/-}$ mice (day 5 p.i.) with either anti-Cxcr2 or IgG antibody. 2 h later, mice received anti-Gr-1 PE and were sacrificed 10 min later. The number of resident (Gr-1^{-}) donor (CFSE^{+}/CD45.1^{+}) neutrophils (CD11b^{+}/Ly6G^{+}) and monocytes (CD11b^{+}/Ly6C^{+}) in the DRG was determined by FACs. Mean (±SEM) of 7–10 mice is pooled from two experiments. (c and d) B6 or IfnαR$^{-/-}$ mice were HSV-1 infected and at day 5 p.i., the DRG stained for Cxcl2. (d) Graphs show Cxcl2 expression of monocytes isolated from the DRG and spleen (individual mice pooled from four experiments). (e) CD11b^{+}Ly6C^{+} monocytes were sorted from DRG or spleen of day 5 HSV-1–infected B6 or IfnαR$^{-/-}$ mice for qPCR. Mean (±SEM) of Cxcl2 mRNA expression is pooled from two experiments. *, $P < 0.05$; **, $P < 0.01$; ***, $P < 0.001$; ****, $P < 0.0001$ (unpaired Student's *t* test).

Type I IFN signaling directly suppresses Cxcl2 production by monocytes, but not neutrophils, in the sensory ganglia

We examined the mechanism by which type I IFN suppresses Cxcl2 expression. We reasoned that IFN may act either directly to suppress chemokine expression or, alternatively, may suppress neutrophil recruitment by acting on factors upstream of Cxcl2. To distinguish between these possibilities, we used mixed BM chimeras, reconstituting irradiated B6.Ly5.1 mice with 50:50 mix of B6.Ly5.1 (CD45.1^{+}) and IfnαR$^{-/-}$ (CD45.2^{+}) BM (Fig. 4 a). We infected chimeras and measured neutrophil recruitment and Cxcl2 expression in the DRG. In line with the full chimeras (Fig. 2 c), the presence IfnαR$^{-/-}$ BM (in this study representing 50% of hematopoietic cells) enabled the recruitment of both wild-type and IfnαR$^{-/-}$ neutrophils into the DRG (Fig. 4 b). Upon examining Cxcl2 expression, we found that although IfnαR$^{-/-}$ monocytes (defined here as

$CD11b^+Ly6G^-$) were actively producing Cxcl2, within the same ganglia, wild-type monocytes showed poor expression of this chemokine. In contrast to monocytes, Cxcl2 production by neutrophil was minimally affected by type I IFN signaling, with B6 and $IfnαR^{-/-}$ neutrophils having equivalent Cxcl2 levels.

Consistent with these in vivo observations, treating BM with IFN-αβ, IFN-γ, or an IFN-αβγ cocktail in vitro, inhibited the

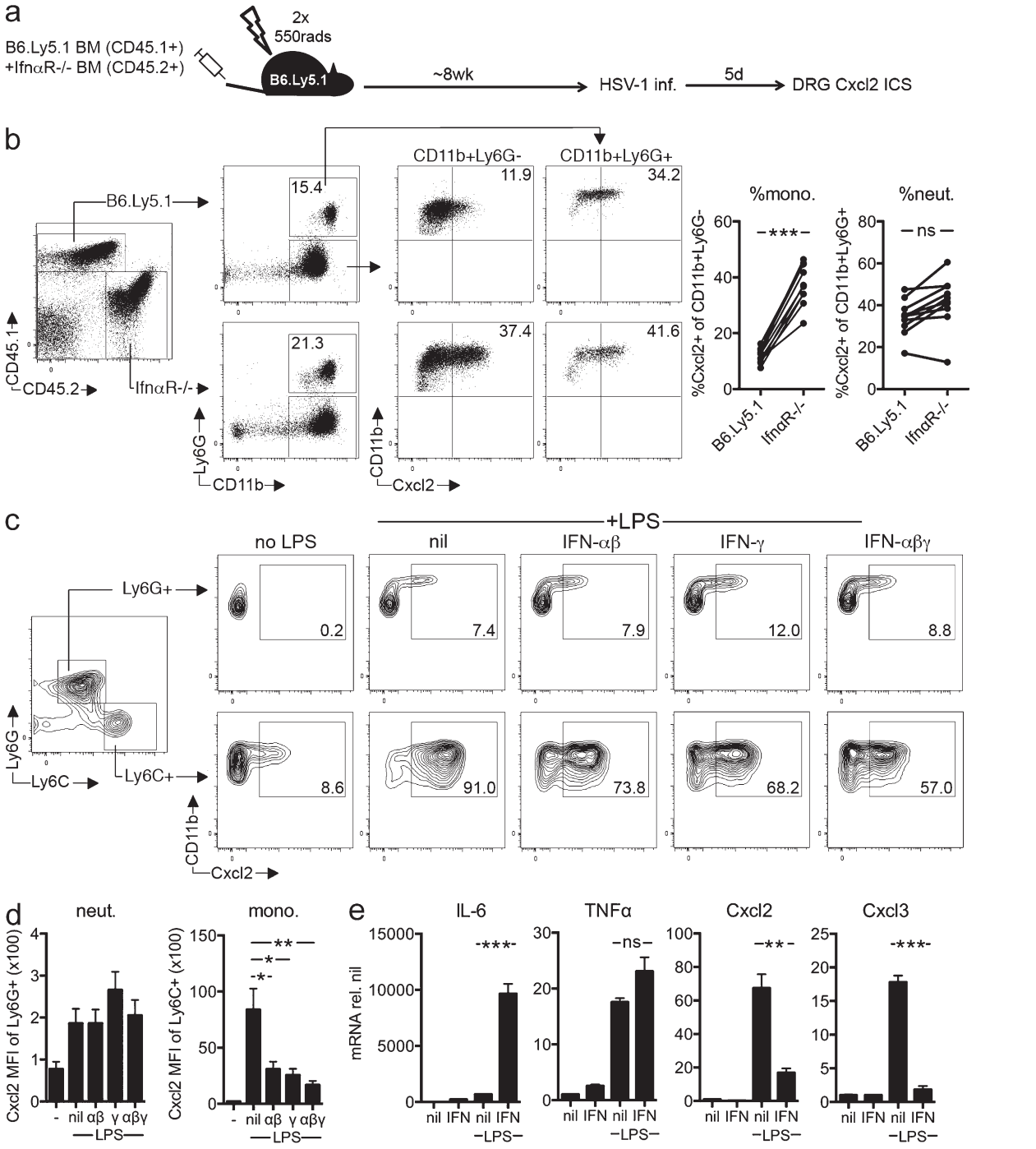

Figure 4. Type I IFN signaling directly suppresses Cxcl2 expression by monocytes. (a and b) Mixed B6.Ly5.1 ($CD45.1^+$) and $IfnαR^{-/-}$ ($CD45.2^+$) BM chimeras were infected with HSV-1 and at day 5 p.i., the DRG analyzed for Cxcl2 expression. Graphs show percentage of $CD11b^+Ly6G^-$ monocytes and $CD11b^+LyG^+$ neutrophils producing Cxcl2 ($n = 10$, pooled from 3 experiments). (c and d) B6 BM was pretreated with IFN-α/β, IFN-γ, or IFN-αβγ before LPS stimulation and stained for Cxcl2 production. (d) Graphs show Cxcl2 MFI ± SEM pooled from three experiments. (e) RAW cells were pretreated with IFN-αβγ before LPS stimulation. 3 h later, mRNA expression was measured by qPCR. Mean (±SEM) expression (relative nil treatment) is pooled from 2–4 experiments. *, $P < 0.05$; **, $P < 0.01$, ***, $P < 0.0001$ (unpaired Student's *t* test).

capacity of Ly6C$^+$ monocytes (but not Ly6G$^+$ neutrophils) to produce Cxcl2 in response LPS (Fig. 4, c and d). Finally, IFN blocked Cxcl2 expression at a transcriptional level as IFN treated RAW cells failed to up-regulate Cxcl2/3 mRNA expression in response to LPS (Fig. 4 e). IFN had no effect on TNF, and augmented IL-6 mRNA expression, demonstrating its selective action. Collectively, these data indicate that IFN signaling suppresses the ability of monocytes, but not neutrophils, to produce the Cxcr2 chemokine ligands within the ganglia. This suppression operates directly in a cell-intrinsic manner, independent of extraneous or upstream factors.

Finally, we examined why type I IFN inhibited Cxcl2 expression and neutrophil recruitment to the DRG, but fails to do so in the skin. This is unlikely to be caused by differential IFN expression between the two sites, as IFN-β (and IFN-γ) was expressed in both skin and DRG after infection (unpublished data). We found that IfnαR$^{-/-}$ mice had moderately, but not statistically significant, elevated neutrophils and Cxcl1/2/3 expression in the skin after HSV-1 infection, whereas showing overall diminished monocyte numbers (Fig. 5, a and b). At a cellular level, IfnαR$^{-/-}$ skin monocytes expressed higher Cxcl2 compared with B6 counterparts, in both straight and mixed BM chimera settings (Fig. 5, c and d). Thus, IFN does appear to limit Cxcl2 expression by skin monocytes. However, it is important to note that this suppression is incomplete, in contrast to the total inhibition seen in the ganglia (Fig. 3). Therefore, it is possible that it is this difference in Cxcl2 shutdown that is the underlying basis for the differential neutrophil infiltration between the two tissues. Additionally, given that the skin and ganglia have distinct cellular compositions, it is also possible that the skin has multiple or distinct cell types capable of recruiting neutrophils, whereas the ganglia is entirely dependent on monocytes to fulfill this role.

Overall, our findings are consistent with several reports of enhanced neutrophilia in the absence of type I IFN after infection with influenza (Shahangian et al., 2009; Seo et al., 2011) and *Listeria* (Brzoza-Lewis et al., 2012) and in tumors (Jablonska et al., 2014). Thus, IFN limits neutrophilia across multiple infections and inflammatory settings. Indeed, a previous study has shown the absence of type I IFN signaling on hematopoietic cells enhanced Cxcl1/2 production by monocytes after influenza infection (Seo et al., 2011). Furthermore, IFN-α has been shown to repress Cxcl1/2 production by BM macrophages in vitro (Shahangian et al., 2009). Therefore, our study in combination with these earlier findings, provide strong evidence that IFN regulates neutrophil recruitment by limiting Cxcl1/2/3 expression by myeloid cells. However, the precise mechanism for how IFN regulates chemokine expression has remained unclear, largely due to the difficulty in distinguishing whether enhanced chemokine expression observed in the absence of IFN

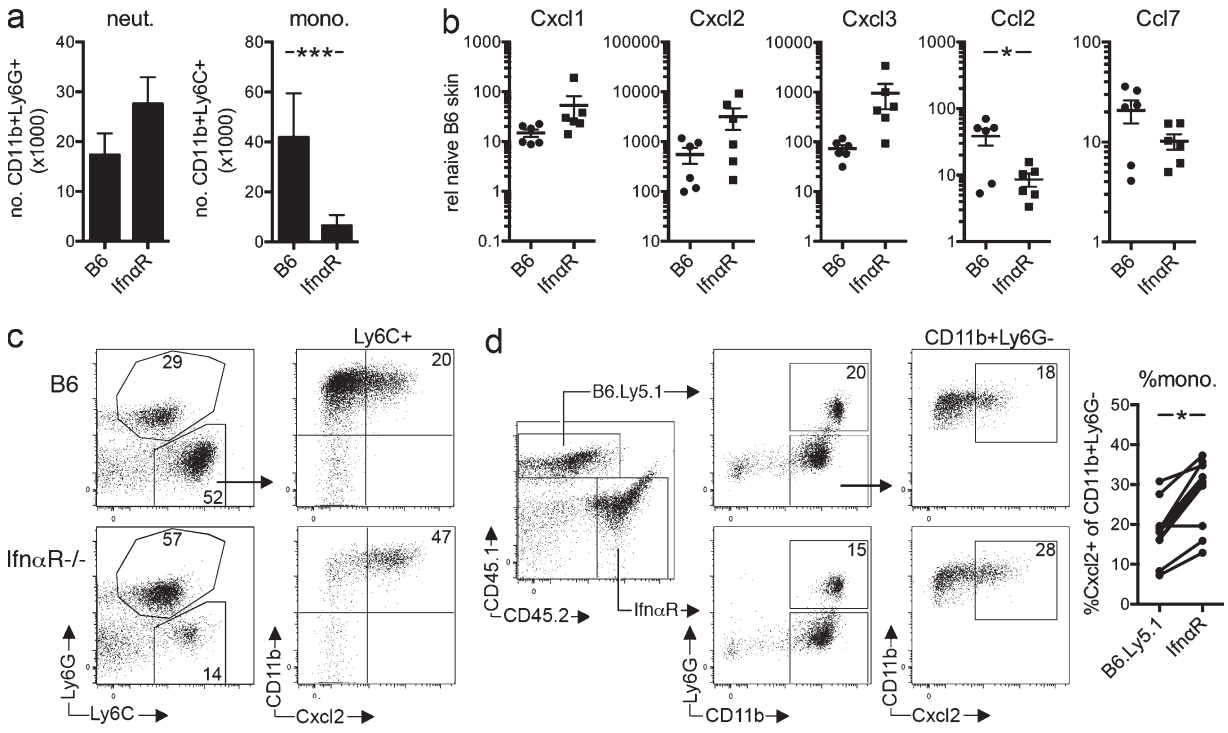

Figure 5. Type I IFN signaling partially limits Cxcl2 expression by skin monocytes after HSV-1 infection. B6 and IfnαR$^{-/-}$ mice were infected with HSV-1 and, 5 d later, the skin was analyzed for (a) neutrophils (CD11b$^+$/Ly6G$^+$) and monocytes (CD11b$^+$/Ly6C$^+$) by FACs (mean ± SEM from 4 experiments, n = 14–15), (b) chemokine expression by qPCR (values are relative to naive B6 skin, individual mice pooled from 2 experiments), or (c) Cxcl2 expression (inset values show mean pooled from 3 experiments, n = 8–10). (d) Mixed B6Ly5.1 (CD45.1$^+$) and IfnαR$^{-/-}$ (CD45.2$^+$) BM chimeras were infected with HSV-1 and at day 5 p.i. the skin was stained for Cxcl2. Values are pooled from three experiments (n = 10). *, P < 0.05; ***, P < 0.0001 (unpaired Student's t test).

is a consequence of uncontrolled pathogen growth and the emergence of upstream factors such as IL-1 (Guarda et al., 2011) or whether IFN was acting specifically to suppress chemokine expression. Here, we provide conclusive in vivo evidence to formally delineate between these possibilities, showing that IFN inhibits the ability of monocytes to produce Cxcl2 in a cell-intrinsic manner.

Why neutrophils are restricted from entering the ganglia remains unresolved; however, it is tempting to speculate that, given their destructive effector functions (Mantovani et al., 2011), restricting neutrophil migration to the DRG may serve to limit neuronal pathology. Indeed, neutrophils are suspected of exacerbating several autoimmune disorders, and consequently, emerging therapies are geared at reducing neutrophil infiltrate (Eyles et al., 2006; Stadtmann and Zarbock, 2012). Therefore, our findings, which provide a mechanistic understanding of how neutrophil recruitment to inflamed tissues is suppressed, may provide insight for such therapies.

MATERIALS AND METHODS

Mice, viruses, and cell lines. C57BL/6 (B6), B6.SJL-PtprcaPep3b/BoyJ (B6.Ly5.1), Balb/C, Rag-common γ chain$^{-/-}$ (Rag-γC$^{-/-}$), CCR2$^{-/-}$, MyD88$^{-/-}$, TLR3$^{-/-}$, IfnαR2$^{-/-}$, and Ifnγ$^{-/-}$ mice were bred at University of Melbourne and used at 6–20 wk of age. Mice were infected with 10^6 PFU KOS (unless otherwise stated) or SC16 strain of HSV-1 by the flank scarification method of inoculation as previously described (van Lint et al., 2004). BM chimeras were generated by irradiation with two doses of 550 rad, 3 h apart, and reconstitution with 10×10^6 donor BM cells. Animal experiments were approved by The University of Melbourne Animal Ethics Committee. RAW264.7 cells were grown in RPMI supplemented with 1 mM sodium pyruvate, 25 mM Hepes, MEM-NEA, 50 µM 2-mercaptoethanol, L-glutamine, antibiotics, and 10% FCS.

Antibodies, flow cytometry, and cell sorting. Anti–mouse CD11b (M1/70), Gr-1 (RB6-8C5), Ly6C (AL-21), Ly6G (1A8), CD45.1 (A20), CD45.2 (104), CD31 (390), and EPCAM (G8.8) directly conjugated monoclonal antibodies (BD or eBioscience) were used for flow cytometry and microscopy. Spleens were prepared by mechanical disruptions, while the skin and dorsal root ganglia (T8-12) were digested in type III collagenase (3 mg/ml; Worthington) with DNase (5 µg/ml; Sigma-Aldrich). Samples were acquired on a Fortessa (BD) and analyzed with FlowJo software. Cell sorting was performed on a FACSAria (BD) and skin cell subsets were sorted into epithelial (CD45$^-$EPCAM$^+$), endothelial (CD45$^-$CD31$^+$), stromal (CD45$^-$EPCAM$^-$CD31$^-$), lymphocyte (CD45$^+$CD11b$^-$), monocyte/macrophage (CD45$^+$CD11b$^+$Ly6G$^-$), and neutrophil (CD45$^+$CD11b$^+$Ly6G$^+$) subsets. For antibody blockade of type I IFN signaling in vivo, mice were injected i.p. with 0.2 mg anti–mouse IfnαR-1 antibody (MAR1-5A3; BioXCell) on days 1, 2, 3, and 4 p.i.

Intracellular Cxcl2 staining. For ex vivo analysis of Cxcl2 expression, tissues were digested in type III collagenase/DNase with Brefeldin A (10 µg/ml; Sigma-Aldrich). Cells were stained with live/dead dye (Invitrogen) and for cell surface antigens, fixed (Cytofix/Cytoperm; BD), and stained with 0.15 µg polyclonal goat anti–mouse Cxcl2 (R&D Systems) or normal goat IgG control in Perm/Wash solution (BD) at room temperature before detection with donkey anti–goat 488 (Life Technologies; Eberlein et al., 2010). For ICS after in vitro stimulation, BM cells isolated from femur and tibia were treated with recombinant mouse IFN-α, β (5,000 U/ml; PBL Interferon) and/or IFN-γ (20 ng/ml; PeproTech) for 2–3 h before LPS (100 ng/ml; Sigma-Aldrich) stimulation for 60 min. Cells were then cultured for a further 4 h in the presence of BFA (10 µg/ml) and stained as above.

Real-time PCR, ELISA, and microscopy. For mRNA expression analysis of tissues, organs were harvested into RNAlater (Invitrogen), RNA extracted using the RNEasy Micro kit (QIAGEN), and cDNA synthesized with SuperScript III Reverse transcription (Invitrogen) using oligo-dT primers (Promega). For sorted and RAW cells, cDNA was prepared using the SYBR Green Gene Expression cells-to-Ct kit (Life Technologies). Quantitative real-time PCR (qPCR) was performed with Fast SYBR Green Master mix (Life Technologies) with primers described in Table S1). For transcriptional analysis, RAW cells were treated with an IFN-αβγ cocktail for 2–3 h before LPS (10 ng/ml) stimulation. 3 h after LPS addition, cDNA synthesis, and qPCR were performed as above. Gene expression was normalized to Gapdh (ΔCT) and values are shown either as target gene mRNA levels relative to Gapdh ($2-\Delta^{CT}$) or further calculated relative to naive tissue ($2-\Delta\Delta^{CT}$). For ELISA, tissues were harvested and homogenized in PBS/0.1% FCS with proteinase inhibitors (Sigma-Aldrich) and Ccl2 (eBioscience) and Cxcl2 (R&D Systems) levels measured in homogenate. For microscopy, tissues were dehydrated (20% sucrose) and frozen in OCT (Tissue-Tek). Sections were fixed and permeabilized in acetone, blocked with serum-free protein block (Dako) and stained with anti-Ly6G, anti-Ly6C, and DAPI. Images were acquired on a LSM700 confocal microscope with Zen 2012 software (both from Carl Zeiss, Inc.) and processed with ImageJ 1.57 Dscho.

Cxcr2 blocking of transferred BM neutrophils/monocytes. For Cxcr2 blocking experiments, femur/tibia BM were isolated from B6.Ly5.1 mice, labeled with 0.1 µM CFSE (Invitrogen) and ∼10×10^6 BM cells resuspended in 50 µg anti-Cxcr2 or IgG2a isotype control antibody (R&D Systems) and transferred i.v. into HSV-infected C57BL/6 or IfnαR$^{-/-}$ recipients. 2 h after transfer, mice were injected i.v. with 3 µg anti–Gr-1-PE and sacrificed 10 min later. Mice were perfused and tissues harvested for flow cytometric analysis.

Statistical analysis. Statistical analysis was performed using unpaired, two-tailed Student's *t* tests.

Online supplemental material. Table S1 shows real-time qPCR primers sequences. Online supplemental material is available at http://www.jem.org/cgi/content/full/jem.20132183/DC1.

This work was supported by the Australian National Health and Medical Research Council and Australian Research Council.

The authors have no conflicting financial interests.

Submitted: 18 October 2013
Accepted: 24 March 2014

REFERENCES

Addison, C.L., T.O. Daniel, M.D. Burdick, H. Liu, J.E. Ehlert, Y.Y. Xue, L. Buechi, A. Walz, A. Richmond, and R.M. Strieter. 2000. The CXC chemokine receptor 2, CXCR2, is the putative receptor for ELR+ CXC chemokine-induced angiogenic activity. *J. Immunol.* 165:5269–5277.

Ashkar, A.A., and K.L. Rosenthal. 2003. Interleukin-15 and natural killer and NKT cells play a critical role in innate protection against genital herpes simplex virus type 2 infection. *J. Virol.* 77:10168–10171. http://dx.doi.org/10.1128/JVI.77.18.10168-10171.2003

Brandes, M., F. Klauschen, S. Kuchen, and R.N. Germain. 2013. A systems analysis identifies a feedforward inflammatory circuit leading to lethal influenza infection. *Cell.* 154:197–212. http://dx.doi.org/10.1016/j.cell.2013.06.013

Brzoza-Lewis, K.L., J.J. Hoth, and E.M. Hiltbold. 2012. Type I interferon signaling regulates the composition of inflammatory infiltrates upon infection with Listeria monocytogenes. *Cell. Immunol.* 273:41–51. http://dx.doi.org/10.1016/j.cellimm.2011.11.008

Butcher, E.C., and L.J. Picker. 1996. Lymphocyte homing and homeostasis. *Science.* 272:60–66. http://dx.doi.org/10.1126/science.272.5258.60

Cyster, J.G. 2005. Chemokines, sphingosine-1-phosphate, and cell migration in secondary lymphoid organs. *Annu. Rev. Immunol.* 23:127–159. http://dx.doi.org/10.1146/annurev.immunol.23.021704.115628

Eberlein, J., T.T. Nguyen, F. Victorino, L. Golden-Mason, H.R. Rosen, and D. Homann. 2010. Comprehensive assessment of chemokine expression profiles by flow cytometry. *J. Clin. Invest.* 120:907–923. http://dx.doi.org/10.1172/JCI40645

Eyles, J.L., A.W. Roberts, D. Metcalf, and I.P. Wicks. 2006. Granulocyte colony-stimulating factor and neutrophils—forgotten mediators of inflammatory disease. *Nat. Clin. Pract. Rheumatol.* 2:500–510. http://dx.doi.org/10.1038/ncprheum0291

Guarda, G., M. Braun, F. Staehli, A. Tardivel, C. Mattmann, I. Förster, M. Farlik, T. Decker, R.A. Du Pasquier, P. Romero, and J. Tschopp. 2011. Type I interferon inhibits interleukin-1 production and inflammasome activation. *Immunity.* 34:213–223. http://dx.doi.org/10.1016/j.immuni.2011.02.006

Halford, W.P., L.A. Veress, B.M. Gebhardt, and D.J. Carr. 1997. Innate and acquired immunity to herpes simplex virus type 1. *Virology.* 236:328–337. http://dx.doi.org/10.1006/viro.1997.8738

Jablonska, J., C.F. Wu, L. Andzinski, S. Leschner, and S. Weiss. 2014. CXCR2-mediated tumor-associated neutrophil recruitment is regulated by IFN-β. *Int. J. Cancer.* 134:1346–1358. http://dx.doi.org/10.1002/ijc.28551

Mantovani, A., M.A. Cassatella, C. Costantini, and S. Jaillon. 2011. Neutrophils in the activation and regulation of innate and adaptive immunity. *Nat. Rev. Immunol.* 11:519–531. http://dx.doi.org/10.1038/nri3024

Ng, L.G., J.S. Qin, B. Roediger, Y. Wang, R. Jain, L.L. Cavanagh, A.L. Smith, C.A. Jones, M. de Veer, M.A. Grimbaldeston, et al. 2011. Visualizing the neutrophil response to sterile tissue injury in mouse dermis reveals a three-phase cascade of events. *J. Invest. Dermatol.* 131:2058–2068. http://dx.doi.org/10.1038/jid.2011.179

Reiss, Y., A.E. Proudfoot, C.A. Power, J.J. Campbell, and E.C. Butcher. 2001. CC chemokine receptor (CCR)4 and the CCR10 ligand cutaneous T cell-attracting chemokine (CTACK) in lymphocyte trafficking to inflamed skin. *J. Exp. Med.* 194:1541–1547. http://dx.doi.org/10.1084/jem.194.10.1541

Sallusto, F., and A. Lanzavecchia. 2009. Heterogeneity of CD4+ memory T cells: functional modules for tailored immunity. *Eur. J. Immunol.* 39:2076–2082. http://dx.doi.org/10.1002/eji.200939722

Seo, S.U., H.J. Kwon, H.J. Ko, Y.H. Byun, B.L. Seong, S. Uematsu, S. Akira, and M.N. Kweon. 2011. Type I interferon signaling regulates Ly6C(hi) monocytes and neutrophils during acute viral pneumonia in mice. *PLoS Pathog.* 7:e1001304. http://dx.doi.org/10.1371/journal.ppat.1001304

Serbina, N.V., T. Jia, T.M. Hohl, and E.G. Pamer. 2008. Monocyte-mediated defense against microbial pathogens. *Annu. Rev. Immunol.* 26:421–452. http://dx.doi.org/10.1146/annurev.immunol.26.021607.090326

Shahangian, A., E.K. Chow, X. Tian, J.R. Kang, A. Ghaffari, S.Y. Liu, J.A. Belperio, G. Cheng, and J.C. Deng. 2009. Type I IFNs mediate development of postinfluenza bacterial pneumonia in mice. *J. Clin. Invest.* 119:1910–1920. http://dx.doi.org/10.1172/JCI35412

Shuster, D.E., M.E. Kehrli Jr., and M.R. Ackermann. 1995. Neutrophilia in mice that lack the murine IL-8 receptor homolog. *Science.* 269:1590–1591. http://dx.doi.org/10.1126/science.7667641

Stadtmann, A., and A. Zarbock. 2012. CXCR2: From Bench to Bedside. *Front Immunol.* 3:263. http://dx.doi.org/10.3389/fimmu.2012.00263

Svensson, M., J. Marsal, A. Ericsson, L. Carramolino, T. Brodén, G. Márquez, and W.W. Agace. 2002. CCL25 mediates the localization of recently activated CD8alphabeta(+) lymphocytes to the small-intestinal mucosa. *J. Clin. Invest.* 110:1113–1121. http://dx.doi.org/10.1172/JCI0215988

van Lint, A., M. Ayers, A.G. Brooks, R.M. Coles, W.R. Heath, and F.R. Carbone. 2004. Herpes simplex virus-specific CD8+ T cells can clear established lytic infections from skin and nerves and can partially limit the early spread of virus after cutaneous inoculation. *J. Immunol.* 172:392–397.

Zlotnik, A., and O. Yoshie. 2012. The chemokine superfamily revisited. *Immunity.* 36:705–716. http://dx.doi.org/10.1016/j.immuni.2012.05.008